International Journal of Physical Sciences Vol. 6(4), pp. 635-640, 18 February, 2011
Available online at http://www.academicjournals.org/IJPS
DOI: 10.5897/IJPS10.487
ISSN 1992 - 1950 ©2011 Academic Journals

Full Length Research Paper

Synthesis and characterization of gold nanoparticles using 1-alkyl, 3-methyl imidazolium based ionic liquids

Madu, A. N.[1]*, Njoku, P. C.[2], Iwuoha, G. N.[3] and Agbasi, U. M.[4]

[1]Crawford University, Faith-City Igbesa, Ogun State, Nigeria.
[2]Federal University of Technology, Owerri, Imo State, Nigeria.
[3]Department of Pure and Applied Chemistry, University of Portharcourt, River State, Nigeria.
[4]Imo State Polytechnic, Ohaji, Owerri, Imo State, Nigeria.

Accepted 18 February, 2011

The formation of gold nanoparticles has been studied via the reduction of the metal salts in different Ionic Liquids (IIs) based on the 1-alkyl-3-methyl-imidazolium cation and different anions. Particles were grown at different temperatures for 24 h. The structure and morphology of the resulting nanomaterials has been studied via wide angle x-ray scattering (WAXS), transmission electron microscopy (TEM), scanning electron microscopy (SEM), and by spectroscopic techniques. Electron microscopic measurements reveal large differences between both the samples grown at different temperatures and in different ILs. The comparison between the different temperatures, but within one IL shows that 1-ethyl-3-methyl-imidazolium methane sulfonate (Emim) (MS) is the most straightforward IL to study in the case of gold nanoparticles. In this IL, the gold particles are always spherical and have a diameter of 5 to 7 nm. The significant change that occurs with increasing temperature is the aggregation of more and more gold particles into relatively well ordered supracrystalline aggregates at 180°C after 24 h. Aggregation with increasing temperature is qualitatively also supported by the UV/Vis data which show a decrease in the surface plasmon band with increasing reaction temperature. The formation of the somewhat larger particles at 140°C could be due to Ostwald ripening. If Ostwald ripening indeed takes place in (Emim) (ES), this suggests that (Emim) (ES) is not able to completely stabilize the small particles with a diameter of only a few nanometers. This is in contrast to (Emim) (MS).

Key words: Nanoparticles, plamons, aggregation, stabilization, monoclinic.

INTRODUCTION

The chemistry of inorganic materials syntheses is mostly dominated by the study of species in solution. Most widely used solvents for modern chemical reaction and materials synthesis are organic compounds that possess potential pollution and toxic implications and in recent times, minimizing pollution has become a major concern for chemical industry. Quite recently, ionic liquids (ILs) have gained a great deal of both academic and industrial attention worldwide as a new class of compounds for a potential effective green replacement of conventional organic solvents for lasting development of human society (Seddon, 2003).

*Corresponding author. E-mail: josalex67@yahoo.com. Tel: +2348066024503. Fax: +23460230450.

Ionic liquids have gained immense advantage in recent time over other solvents in the synthesis of inorganic materials due to their enormous characteristics. They provide a medium which appear to be capable of dissolving a vast range of inorganic molecules to high concentrations. Most widely used solvents for modern chemical reactions and material syntheses are organic solvents having potential pollution and toxic implications and so as a green recyclable alternative to traditional organic solvents, ionic liquids have shown promise in minimizing these obvious implications. Ionic liquids are organic salts that contain essentially only ions with low melting point. Some ionic liquids are in dynamic equilibrium where at any time, more than 99.99% of the liquids are made up of ionic rather than molecular species.

Their melting points fall below 100°C and at times as

lows as -98°C (Seddon et al., 2000). Advantages of ionic liquids over conventional liquids also include some attractive physicochemical properties such as negligible vapour pressure even at elevated temperatures, excellent chemical stability, and high ionic conductivity up to 0.10 S cm^{-1}, high mobility, high heat capacity, high cohesive energy density, low toxicity and non-inflammability among others (Hagiwara and Costa, 2006).

The synthesis and functionalization of gold nanoparticles modified with ionic liquids based on the imidazolium cation has been reported (Ito and Naka, 2004). The obtained gold nanoparticles can be used as exceptionally high extinction dyes for colorimetric sensing of anions in water via particle aggregation process.

Gold and platinum nanoparticles with diameters of 2 to 3.5 and 2 to 3.2 nm, respectively, can also be synthesized using novel thiol-functionalized ionic liquids (TFILs). TFILs act as a highly effective medium for the preparation and stabilization of gold and platinum nanoparticles, thus becoming highly dispersible in aqueous media (Kim et al., 2004).

The synthesis of a new gold nanoparticles (AuNPs) in an amine-functionalized ionic liquid (AFIL) 1-(3-aminopropyl) 3-butyl imidazolium chloride (AmPrBIM)Cl and its application as building block in nanotechnology has been successfully achieved (Mecerreves et al., 2007). The TEM image of the AuNPs stabilized by AFIL illustrates the formation of spherical particles with average diameters of 33 nm. The direct aqueous synthesis of large gold nanoparticles using alkyl-thiosulphates (Bunte Salt) have been reported (Dahl, 2008). The size dependent electronic and optical properties of interest in gold nanoparticles have generated interest in gold particle-based devices including microelectronic and optical devices as well as in vitro sensors. Gold nanoparticle, (AuNPs) smaller than 2.0 nm in diameter may display non-linear current Vs voltage behaviour at room temperature while those larger than 5.0 nm in diameter possesses strong optical properties due to the resonant behaviour between visible light and surface electrons (Plasmons), characterized by an optical absorbance at 520 nm.

The Brust method (Dahl, 2008) provides a direct synthesis route which imparts control over both functionality and size. While ligand exchange reactions allows for modification of existing nanomaterials post synthesis. However, both methods have significant drawbacks that limit their utility in the general synthesis of functionalized AuNPs. The Brust preparation is most effective in the synthesis of AuNPs less than 5.0 nm in diameter while nanoparticles greater than 5.0 nm in diameter are typically synthesized using charged ligands such as citrate 76 or tetraoctylammonium bromide (TOAB), making the introduction of certain ligands (e.g. thiols) during ligand exchange challenging. Recently the use of alkyl-thiosulphates-Bunte Salts (Murray et al., 2000) alternatives to functionalized thiols for the direct synthesis of gold nanoparticles has been proposed (Murray et al., 2000).

Functionalized Bunte Salts are synthetically straighter forward to prepare than most functionalized thiols and can be stored for a long period without oxidizing to disulphide when used in gold nanoparticle synthesis, the Bunte Salt first physically adsorbs to the surface of the developing nanoparticle and then eliminates sulphite to form a thiolate linkage to the gold core.

In a reported work on direct aqueous synthesis of large gold nanoparticles using Bunte Salts (Dahl, 2008) it served as a ligand precursor and can be utilized in the synthesis of gold nanoparticles as large as 9.0 nm while simultaneously imparting a number of hydrophilic functionalities to the surface of the particles, including neutral, cationic and anionic moieties. The Gold nanoparticles were synthesized by reducing Au (III) with sodium borohydride ($NaBH_4$) in the presence of the Bunte Salt. As a capping agent, Bunte Salt act in a manner similar to thiols while possessing the advantages of easy preparation, shelf stability and versatility.TEM analysis of the purified particle solutions supports the size trend suggested by the UV data at the lower (L: Au = ligand) ratios, the synthesized nanoparticles are larger than 5.0 nm in core diameter.

EXPERIMENTALS

In the synthesis of gold nanoparticles, a simple reducing agent: Glycerol was used in a set of ILs based on the same cation (1-ethyl-3-methyl-imidazolium) and three different anions, namely triflate ([Emim)[OTf)), methanesulfonate ([Emim)[MS)) and ethyl sulfate ([Emim)[ES)). The choice of glycerol as reducing agent is informed by the fact that its use in ILs for the preparation of gold nanoparticles has only rarely been studied. In a typical synthesis, 20 mg $HAuCl_4.3H_2O$ was dispersed in 1 g of IL followed by addition of 20 mg of glycerol. The mixture was stirred magnetically and heated at temperature for 24 h. The macroscopic precipitate was isolated by centrifugation and washing with water and ethanol respectively and drying at 60°C.

Instruments and characterization

Wide angle X-ray diffraction (XRD) was done on an ENRAF Nonius FR 590 diffractometer with a Cu K_α X-ray tube fitted with an Inel CPS 120 hemispherical detector ranging from 1 to 120°; 2θ. SAXS curves were recorded at room temperature with a Nonius rotating anode instrument (4 kW, Cu K_α) with pinhole collimation and a MARCCD detector (pixel size: 79). For IR and RAMAN, the FT-IR spectra of the solid samples were recorded from KBr pellets in the same spectral range on a Thermo Nicolet Nexus™ 670 spectrometer. For UV-VIS, the Agilent 8453 spectrometer with 10 mm quartz cuvettes was used. TEM and SEM images were acquired on a Zeiss EM 912 at an acceleration voltage of 120 kV.

RESULTS

Gold nanoparticles were grown in the ILs 1-ethyl-3-methylimidazolium triflate ([Emim] [OTf]), methane

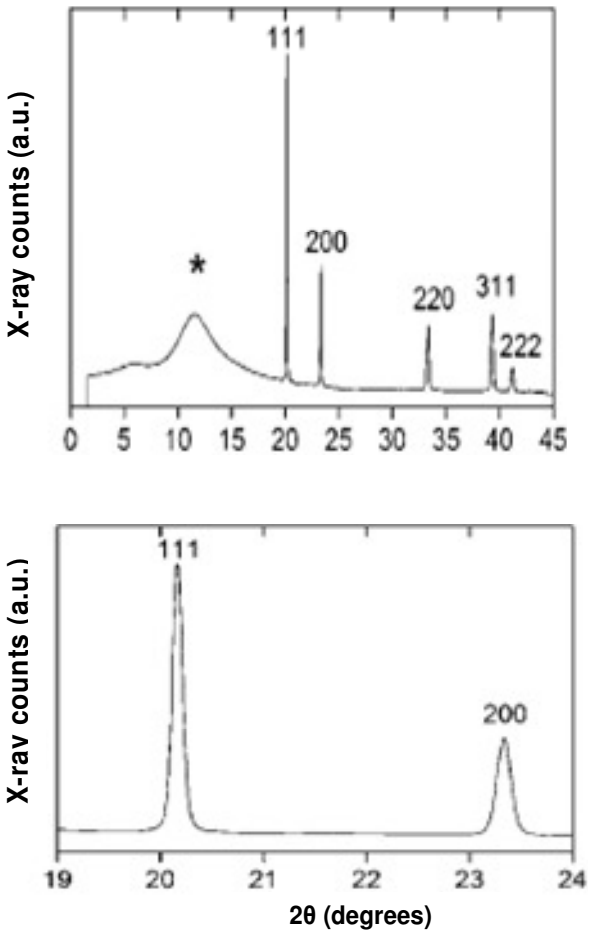

Figure 1. XRD pattern of gold nanoparticles grown in [Emim] MS at 140°C for 24.

sulfonate ([Emim] [MS]), and ethyl sulfate ([Emim] [ES]) via the reduction of Au(III) ions by glycerol at temperatures between 120 and 180°C. The main goal of the study is an evaluation of anion effects on the formation of gold nanocrystals, as anions in ILs have been postulated as one of the key parameters affecting (inorganic) reactions in Ils (Redel et al., 2008). The Wide angle X-ray scattering (WAXS) pattern of a sample grown in [Emim] [MS] at 140°C for 24 h. shown in Figure 1, reveals that there is no difference between the particles grown at different temperatures and in different ionic liquids.

In Figure 2 shows the representative transmission electron microscopy (TEM) images of gold nanoparticles grown in (Emim) (ES) between 120 and 180°C. At 120°C, particles have broad size distribution, a mean diameter of ca. 20 nm, and roughly spherical shapes. Figure 3 shows the TEM images of gold nanoparticles grown in (Emim) (MS) while that grown in (Emim)(OTf) are shown in Figure 4.

Figure 5 shows the UV-Vis spectra of samples grown in (Emim) (MS) and (Emim) (OTf) at different temperatures.

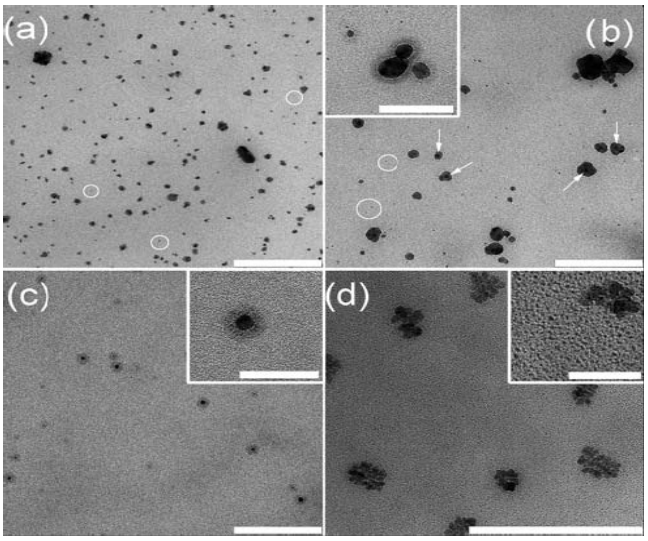

Figure 2. TEM bright field image of gold nanoparticles grown in (Emim) (ES) at (a) 120, (b) 140, (c) 160, and (d) 180°C. Circles highlight particles of about the same sizes and arrows point to the black dots. Insets in (b) and (c) show the presumed IL around the particles. Insets in (d) shows the small particles in the background.

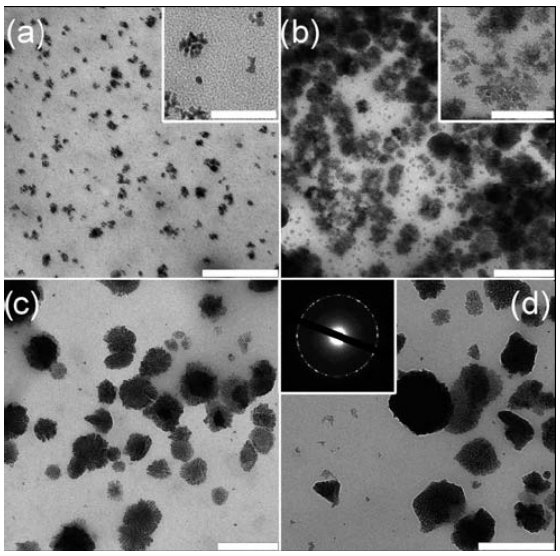

Figure 3. TEM bright field image of gold nanoparticles grown in (Emim) (MS) at (a) 120, (b) 140, (c) 160, and (d) 180°C. Insets in (a) and (b) are higher magnificication images of the aggregates. Insets in (d) is a SAED pattern confirming the polycrystalline nature of the sample.

The samples grown in (Emim) (ES) exhibit too strong absorptions even at very low dilutions and the spectra could not be interpreted conclusively. Arrows indicate plasmon bands; x denotes additional band between 550 and 600 nm.

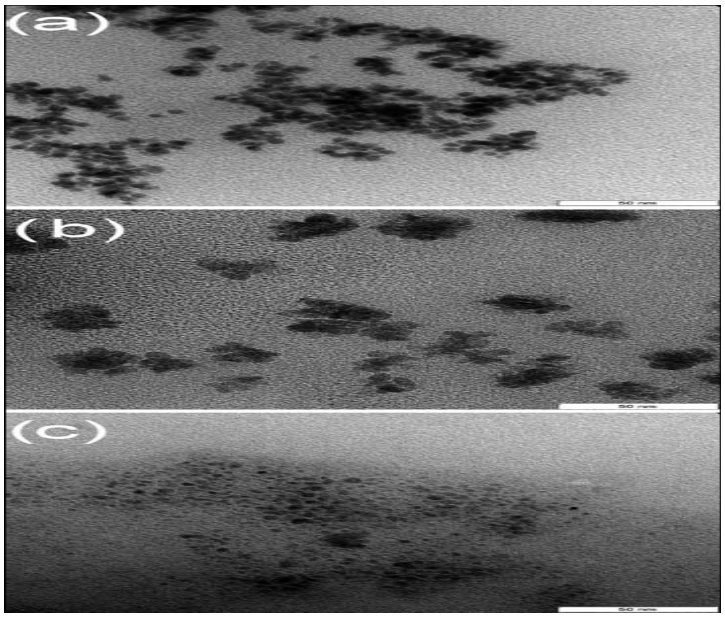

Figure 4. TEM bright field images of gold nanoparticles grown in (Emim) (OTf) at (a) 120, (b) 160, and (c) 180°C.

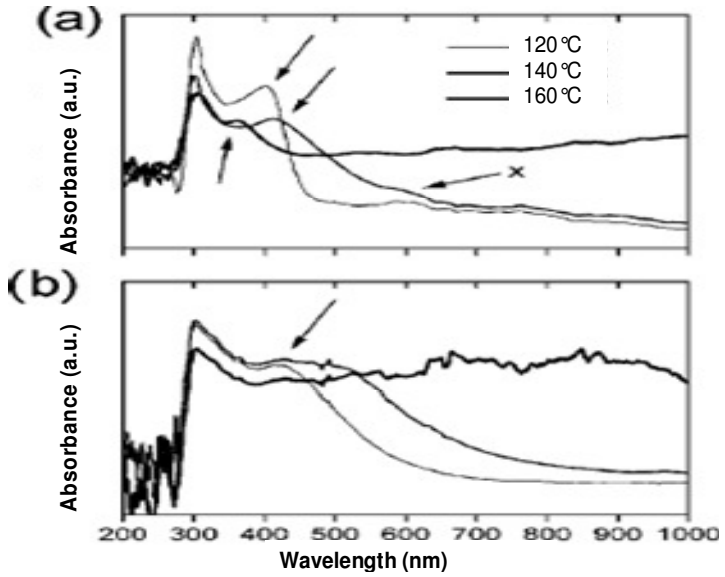

Figure 5. UV/Vis spectra of samples grown in (a) (Emim) (MS) and (b) (Emim) (OTf) at different temperatures. Arrows indicate plasmon bands; x denotes additional band between 550 and 600 nm.

DISCUSSION

The wide angle x-ray scattering (WAXS) pattern of a sample grown in (Emim) (OTf) at 140°C for 24 h is presented in Figure 1. All peak positions can be assigned to face centered cubic (fcc) gold (JCPDS 04-0784). The (111) reflection is more intense than expected for spherical particles and, correspondingly, the (200)/(111) and (220)/(111) intensity ratios are lower than the values reported for bulk, isotropic gold samples (0.52 and 0.32, JCPDS 04-0784). This suggests that the resulting gold particles are dominated by (111) facets. Usually, a high (111) reflection intensity and the absence of other reflections indicate the presence of plate-like crystals with

large (111) facets. However, similar to earlier report (Li et al., 2008), we also observe other reflections than (111). XRD therefore indicates that the samples are not (or not entirely) plate-like, but rather have other morphologies that are dominated by (111) facets. The representative transmission electron microscopy (TEM) (Figure 2) images of gold nanoparticles grown in (Emim) (ES) between 120 and 180°C, respectively reveals that at 120°C, particles with a broad size distribution, a mean diameter of ca. 20 nm, and roughly spherical shapes form. The fact that a large number of the particles are (partly) electron transparent, could, however, also indicate that the particles have an oblong or flattened shape such that they can be considered disk-like rather than egg-like. This assumption is consistent with the observation that also here, the (111) signal in XRD is more pronounced than what is expected for entirely spherical particles. At 140°C, the particles are larger with a mean diameter of 40 to 50 nm. They also appear to be plate or disk-like rather than entirely spherical. The samples grown at 140°C also show a second particle population of small particles with a diameter of only a few nm. The samples grown at 160°C are strikingly different from the earlier two samples in that they exhibit relatively monodisperse, spherical samples with a mean diameter of ca. 15 nm. Moreover, these particles are not, like many of the particles obtained at lower temperatures, aggregated. Much rather, they are uniform and no other particles with different sizes and shapes can be observed. Interestingly, these particles also exhibit a ‘‘ring’’ around each particle, suggesting that here, some IL is still adsorbed on the surface of each particle. At 180°C, TEM shows two particle populations, one with an average diameter of ca. 3 to 4 nm, the larger one with a particle diameter of ca. 15 nm. However, TEM also shows that the reaction temperature is an important parameter to control the shape, size, and aggregation process of the particles. Figure 3 shows TEM data of the samples grown in (Emim) (MS). Unlike the samples previously described, where TEM suggests that individual crystalline particles with more or less well-defined particle morphologies form, the particles observed here appear to be very small (ca. 5 nm) regardless of the reaction temperature. Interestingly, however, the aggregation of the particles changes with reaction temperature. While at 120°C, relatively small aggregates with an overall diameter between ca. 20 and 50 nm, at 160 and 180°, the aggregates become larger and reach well over 200 nm at 180°C. At 160°C, they have a sponge-like appearance, while at 180°C, the aggregates assume shapes that are reminiscent of crystalline organization.

In Figure 4, we show the corresponding TEM images of nanoparticles grown in (Emim) (OTf). At 120°C, individual particles and larger aggregates coexist. At 140 and 160°C, the particles appear somewhat larger and TEM suggests that they are aggregated somewhat more strongly than at 120°C. At 180°C, the individual particles are again rather present as individual particles and TEM shows that there is a small spacing between each particle. This suggests that also here, the particles could be covered with a thin IL layer, although it is (unlike in the above examples) not visible in the TEM.

UV/Vis spectroscopy has been used to confirm that the aggregation observed in TEM is a real representation of the state in the IL dispersion. UV/Vis spectra of (Emim) (MS) (Figure 5), exhibit well-defined absorption bands, which can be assigned to the surface plasmon of the gold nanoparticles (Dahl, 2008).The fact that the bands are relatively narrow supports TEM in that both UV/Vis and TEM show that the particles have a rather narrow size distribution. The spectra of the samples synthesized at higher temperatures occasionally exhibit additional broad humps between 600 and 900 nm. These signals could be due to a contribution of a fraction of particles with other shapes than spherical (Taubert et al., 2008). This is consistent with TEM, which shows that the samples grown in (Emim) (MS) contain particles with morphologies other than small spheres.

Conclusion

The comparison between the different temperatures, but within one IL shows that (Emim) (MS) is the most straightforward IL to study in the case of gold nanoparticles. In this IL, the gold particles are always spherical and have a diameter of 5 to 7 nm. The significant change that occurs with increasing temperature is the aggregation of more and more gold particles into relatively well ordered supracrystalline aggregates at 180°C after 24 h. Aggregation with increasing temperature is qualitatively also supported by the UV/Vis data which show a decrease in the plasmon band with increasing reaction temperature In contrast to particles obtained in (Emim) (MS), particles grown in (Emim) (ES) exhibit a range of sizes and shapes as the reaction temperature increases At 120°C, particles have a relatively broad size distribution form. At 140°C, many particles are larger than at 120°C (ca. 50 nm vs. ca. 20 nm), a further population of much smaller particles with a diameter of only ca. 5 nm is observed. In a sense, TEM suggests that either two distinct populations with clearly different sizes form, or that a second nucleation event takes place, which leads to the small particles observed in TEM. The observation of a second particle generation has been observed before, although in aqueous solution (Taubert et al., 2002) and to the best of our knowledge, there has so far been no evidence of such a process in ILs. Alternatively, the small particles present at 140°C could be identical to the particles at the lower end of the particle size distribution of the sample synthesized at 120°C. In this case, the formation of the somewhat larger particles at 140°C could be due to Ostwald ripening. If Ostwald ripening indeed takes place in (Emim) (ES), this

suggests that (Emim) (ES) is not able to completely stabilize the small particles with a diameter of only a few nanometres. This is in contrast to (Emim) (MS).

REFERENCES

Seddon KR (2003). Ionic Liquids: A taste of the Future. Nat. Mater., 2: 363-368.

Seddon KR, Stark A, Torres MJ (2000). Templated electrodeposition of Silver nanowires in a nanoporous polycarbonate membrane from a non-Aqueous ionic Liquid electrolyte. J. Pure Appl. Chem., 72: 2275-2278.

Hagiwara N, Costa D (2006). Modeling of Optical Response of Gold Nanoparticles. J. Electrochem. Soc. Pennington. N.J., pp. 802–813.

Ito Y, Naka C (2004). Nanochemistry aspects of Titania in dye-sensitized solar cells (DSSCs). Bull. Chem. Soc., 126: 14943-14948.

Kim SK, Demberelnyamba D, Le H (2004). Synthesis and characterization of a size-selective Gold and Platinum nanoparticles using a thiol-Functionalized ionic liquid. Langmuir., 20: 556-559.

Mecerreves D, Rebecca M, Anne-Laure P, Chris T, Markus D, Josetxo P, Hans G, Iñake Z, Iñake M (2007). New amine functional ionic liquid as building block in nanotechnology. Oral Presentation, CIDETEC, Sebastian, 20018.

Dahl JA (2008). Synthesis and characterization of large gold nanoparticles using Bunte Salt. PhD Oral Thesis.

Murray CB, Kagan CR, Bawendi CR (2000). Synthesis and characterization of monodispersed nanocrystals and close-packed nanocrystal assembly. Ann. Rev. Mater. Sci., 30: 545-610.

Redel E, Waltar M, Thomann R, Volmer C, Leith H, Scheerer H, Kruger M, Janaik C (2008). Synthesis, stabilization, functionalization and DFT calculations of Gold nanoparticles in flourous phase (PTFE and ionic liquids). J. Inorg. Chem., 47: 14-16.

Li X, Cheng W, Zhan Q (2008). Chemically derived ultrasmooth grapheme nanoribbon semiconductors. Science, 319: 5867-5872.

Taubert A, Wiesler VM, Mullen K (2008). Dendrimer templated construction of silver nanoparticles. J. Mater. Chem., 13: 22-28.

Taubert A, Li Z (2002). Synthesis, stabilization, functionalization and DFT calculations of Synthesized caloxarenes. Daltons Trans., 19: 723-727.